Journal of Nano- and Electronic Physics
Vol. **7** No 4, 04028(3pp) (2015)

Журнал нано- та електронної фізики
Том **7** № 4, 04028(3cc) (2015)

Influence of Order of Double Step Implantation of $^{64}Zn^+$ and $^{16}O^+$ Ions into Si on Formation of Zinc-containing Nanoparticles

K.B. Eidelman[1,*], K.D. Shcherbachev[1], N.Yu. Tabachkova[1], A.V. Goryachev[2], D.M. Migunov[2], D.A. Dronova[2]

[1] *National University of Science and Technology «MISiS»*
[2] *National Research University of Electronic Technology (MIET)*

(Received 25 September 2015; published online 10 December 2015)

This paper presents the research the formation of zinc-containing nanoparticles (NPs) in Si (001) after double-step hot implantation of $^{64}Zn^+$ and $^{16}O^+$ ions. High-resolution Transmission Electron Microscopy (HRTEM) and X-ray Diffraction (XRD) methods were used to study a crystal structure of the samples. Depth profiles of implanted impurity atoms were measured by Secondary Ion Mass Spectrometry (SIMS). Zn NPs with a size of 3 up to 50 nm were found in the implanted samples. Zinc-containing NPs with the size of 5-10 nm were found in the surface layer of as-implanted Si substrates. The effect of the order of implantation on structural defects and the impurity atoms depth profiles is established.

Keywords: Zn nanoparticles, Double-step ion implantation, Phase formation.

PACS numbers: 61.72.Up, 61.72.Yx

1. INTRODUCTION

Recently, an investigation of metal nanoparticles (NPs) has become popular. Quantum nanoscale effects in metal NPs cause an increased interest in this type of materials in terms of development of high-speed UV photodetectors. Until now, a few methods for synthesizing of NPs on (or inside) substrates exist: chemical vapor deposition by using metalorganic compounds [1], the molecular epitaxy [2], ion implantation [3], the sol-gel method [4], and etc. Among these methods, an ion implantation is considered as one of the cleanest and most flexible methods of producing of composite materials.

Zinc-containing NPs are good wide-gap semiconductors (3-6 eV). For example, ZnO (3.37 eV) is considered as a promising material for optoelectronics, particularly to ultraviolet (UV) laser emitters of a next generation [5, 6]. In addition, it also shows the photoluminescence (PL) in the visible range of a spectrum, due to a presence of intrinsic defects [7, 8]. Zn_2SiO_4 is also an important material used as luminophores for emitting devices, due to its unique properties of luminescence, a wide-band gap (5.5 eV), and an excellent chemical stability [9, 10].

Research of the materials implanted by metal impurities, in particular, zinc, are carried out quite intensively [3, 4], especially, by using a heat treatment in different variations. The heat treatment is used for nucleation and growth of metal and metal-oxide NPs [2]. The NPs, were synthesized by ion implantation, are usually located in the surface region of the substrate [11, 12]. The aim of this work was to study the NPs formation by double-step implantation of Zn^+ and O^+ ions, and to determine an effect of an implantation order on the process.

2. EXPERIMENTAL DETAILS

Two pieces (sample #3 and #4) of n-type Cz-Si(001) single crystal wafer were implanted with $^{64}Zn^+$ and $^{16}O^+$ ions. The SRIM software was used to determine conditions of the double-step implantation. Sample #3 was implanted first with O^+ ions with an energy E of 35 keV, and a fluence D of 5×10^{16} cm^{-2}), and then with Zn^+ ions ($E = 120$ keV, $D = 5 \times 10^{16}$ cm^{-2}). Sample #4 was implanted in an inverse order (Zn^+ (120 keV, 5×10^{16} cm^{-2}) and O^+ (35 keV, 5×10^{16} cm^{-2})). Ion beam with a current density of 50 nA/cm^2 and a diameter of 2 mm canned over the substrate surface at an angle of 7°. Overheating of the samples compared with the room temperature does not exceed 50 degrees due to a low ion current. To avoid amorphization during the implantation, a target was heated up to a temperature of 350-400 °C.

The formation of zinc-containing NDs was studied by using a high-resolution electron microscopy (HRTEM), an X-ray diffraction (XRD) and a secondary ion mass spectroscopy (SIMS) methods. XRD measurements in an out-of-plane grazing-incidence (GID) geometry were performed using by D8 Discover X-ray diffractometer (Bruker Corp.) equipped by 2 kW sealed X-ray tube with copper anode (λ Cu_{K_α} = 1.5406 Å). Diffraction patterns were measured by 2θ detector scan at a fixed position of the sample. An incidence angle of 100 μm beam was of 0.3°. A long Soller slit was set in front of a detector.

A high-resolution electron microscopy (HRXTEM) in combination with electron diffraction and energy dispersive microanalysis (EDAX) by electron microscope JEM-2100 at an accelerating voltage of 200 kV was used to characterise a structure of the damaged layer. The samples were prepared in a cross section.

The depth distribution of implanted impurities was determined by SIMS using on time- flight secondary ion mass spectrometer TOF-SIMS-5. Sputtering was performed using O^+ [2] or Cs^+ ion guns with energy about 1 keV and value of current about hundreds of nA. The size of the spattering beam is about 300×300 mkm^2.

* eidelman@live.ru

Heavy ions of Bi^+ ions with a mass of 209 a.m.u. with energy up to 30 keV were used for the analysis. It allows one to get a high sensitivity for analysis of approximately all heavy ions. The value of Bi^+ ions beam current of the ion beam Bi in impulse did not exceeding 1 pA, an impulse duration was of 1 ns.

3. RESULTS AND DISCUSSION

The process of ion implantation into semiconductors is accompanied by a generation of radiation-induced point defects into a semiconductor substrate. A cascade of collisions caused by an impinging ion forms within $\sim 10^{-12}$ s a disordered region that is highly supersaturated with vacancies and intrinsic interstitial atoms. This disordered region is unstable. Immediately after its formation, the processes of spatial separation of the vacancies and interstitial atoms begin, which is accompanied by the quasi-chemical reactions of these defects with one another and also with other imperfections of the crystal lattice. It can be assumed that these secondary processes can influence on formation of NPs.

XRD revealed zinc NPs in both samples. The measurements were performed in a low resolution in an out-of-plane grazing-incidence (GID) geometry. In sample #4 peak of zinc is better defined, as compared with the sample #3 (Fig. 1). It indicates the difference in size of Zn NPs. The size of these NPs in sample #4 is larger (30 nm) than in sample #3 (12 nm). Perhaps, other zinc-containing phases can exist, but their presence cannot be confirmed due to a weak intensity at the background level.

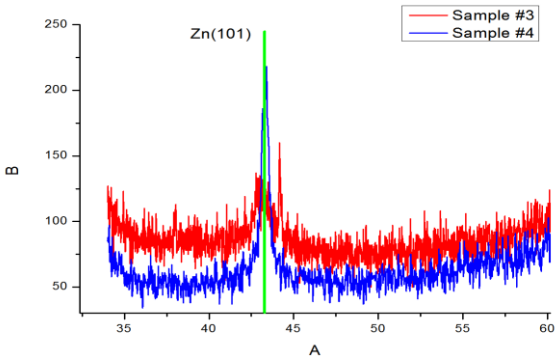

Fig. 1 – GID XRD patterns for the studied samples

Reciprocal space maps (Fig. 2) near reflection Si(004) were measured by high-resolution X-ray diffraction. The intensity of X-ray diffuse scattering is greater in sample #4 rather than in sample #3. It evidences sample #4 contains more defects than sample #3. Both samples have a damaged surface layer of the crystalline quality that has a lattice parameter larger than the Si matrix one. This layer yields a coherent diffraction, which can be seen in the maps as a narrow strip along [001] (Fig. 2). The results show that the ensemble of radiation defects depends on the order of implantation. Apparently, it depends on the occurrence of quasi-chemical reactions between the implanted impurity and radiation-induced matrix point defects.

The damaged surface silicon layer with thickness of about 250nm and with high concentration of radiation defects is clearly visible in TEM image (Fig. 3). Due to the "hot" implantation (temperature substrate of about

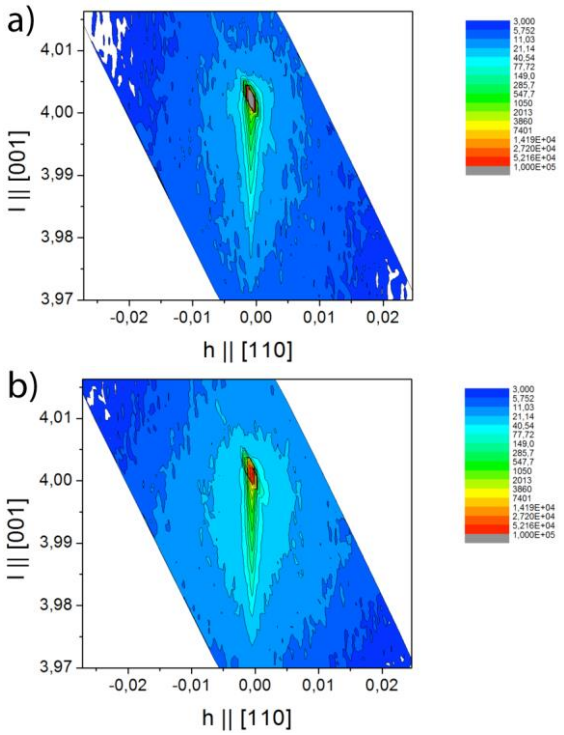

Fig. 2 – Si (004) reciprocal space maps for sample #3 (a) and #4 (b)

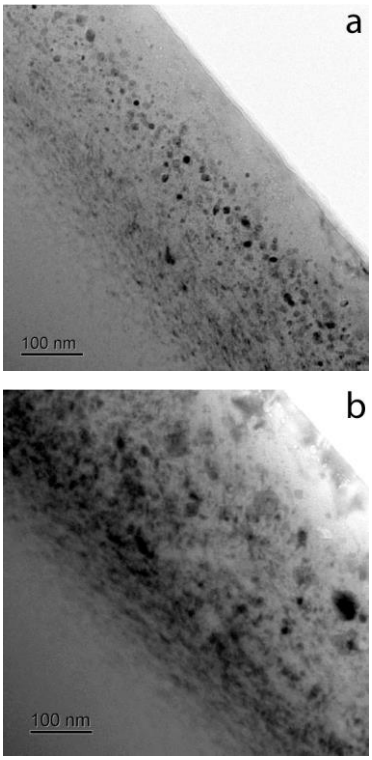

Fig. 3a, b – Bright field cross-section images of the samples #3 (a) and #4 (b)

350-400 °C), the amorphized layer is not seen. Zn NPs, which are coherent with the silicon substrate, formed in the surface silicon layer. Furthermore, in the both samples at a depth of 35 nm zinc-containing NPs with different nature of formation than the NPs Zn are present.

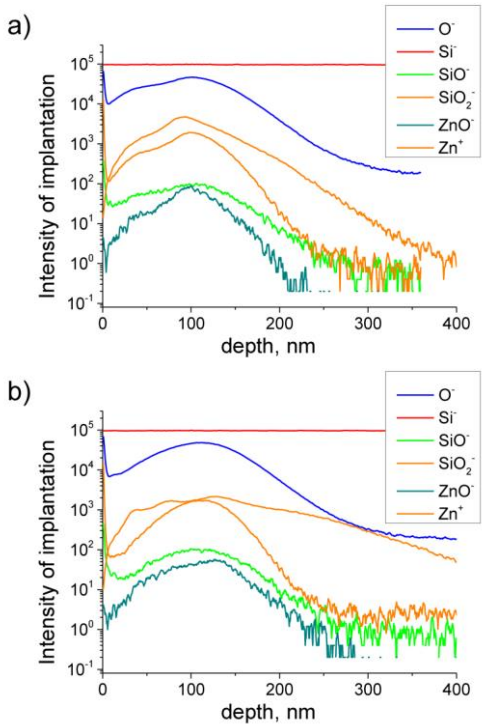

Fig. 4 – The depths profiles of implanted impurities, obtained by TOF-SIMS for sample #3 (a) and #4 (b).

In the sample #4, NPs of Zn are located at a depth of 130 nm (Fig. 3a). NPs size is from 3 to 15 nm. Near to the surface, at a depth of 35 nm arranged zinc-containing NPs with a size of about 5 nm are present. More detailed phase identification phase requires further research. In the sample #4, due to different order of implantation, NPs of Zn are located deeper (170 nm) and their size varies from 10 to 50 nm (Fig. 3b). Zinc-containing NPs with a size of about 10 nm are located at the same depth as in sample #3 (35 nm).

In addition, the impurity depth profiles were measured by TOF-SIMS. Fig. 4 shows the profiles of impurities and dissociated ions. The presence of ions ZnO^- ions hardly indicates the existence of ZnO NPs in the layer, because ZnO phase was not detected by other methods. With the highest probability, the phase of Zn_2SiO_4 is present in the samples, and SIMS reveals parts of Zn_2SiO_4 molecules that dissociated into molecular compounds ZnO^- and SiO_2^-during sputtering.

An impurity implanted first, goes deeper and has several intensity peaks after the second implantation. It can be because the fact that the second implantation is performed into the matrix enriched by a large amount of the implanted impurity atoms and the residual radiation defects.

4. CONCLUSION

As a result of a double-step ion implantation of $^{64}Zn^+$ ($E = 120$ keV, $D = 5 \times 10^{16}$ cm^{-2}) and O^+ ($E = 35$ keV, $D = 5 \times 10^{16}$ cm^{-2}) in the substrate of single crystal Si(001) substrate, heated up to 350 °C, NPs of metal Zn in sizes from 3 to 50 nm are formed. These Zn NPs are coherent with the silicon matrix. TEM shows the presence of smaller zinc-containing particles having a different nature of formation. More detailed phase identification requires the further research. Dimensions of Zn NPs, obtained by TEM and XRD are in a good agreement. The crystalline quality of the damaged layer depends on the order of implantation. Different shape of impurity depth profiles depending on the order of implantation was established by TOF-SIMS. The second implantation leads to a spatial redistribution of the impurity implanted first.

ACKNOWLEDGMENTS

The work was supported by the Ministry of Education and Science (GC № 02.G25.31.0059 from 04.08.2013). The experimental part of the work performed on the equipment, and CCU MCT ECB MIET.

REFERENCES

1. Shu-Cheng Chin, Chun-Yung Chi, Yen-Cheng Lu, Lin Hong, Yu-Li Lin, Fang-Yi Jen, C.C. Yang, Bao-Ping Zhang, Yusaburo Segawa, Kung-Jen Ma, Jer-Ren Yang, *J. Cryst. Growth* **293**, 344 (2006).
2. D.C. Look, D.C. Reynolds, C.W. Litton, R.L. Jones, D.B. Eason, G. Cantwell, *Appl. Phys. Lett.* **81**, 1830 (2002).
3. A.l. Meldrum, Richard F. Haglund Jr., Lynn A. Boatner, C. Woody White, *Adv. Mater.* **13**, 1431 (2001).
4. G. De, L. Tapfer, M. Catalano, G. Battaglin, F. Condlla, P. Mazzoldi, R.F. Haglund, *Appl. Phys. Lett.* **68**, 3820 (1996).
5. S. Chu, M. Olmedo, Z. Yang, J.Y. Kong, J.L. Liu, *Appl. Phys. Lett.* **93**, 181106 (2008).
6. S.L. Cho, J. Ma, Y.K. Kim, Y. Sun, G.K.L. Wong, J.B. Ketterson, *Appl. Phys. Lett.* **75**, 2761 (1999).
7. K. Vanheusden, W.L. Warren, C.H. Seager, D.R. Tallant, J.A. Voigt, B.E. Gnade, *J. Appl. Phys.* **79**, 7983 (1996).
8. K. Vanheusden, C.H. Seager, W.L. Warren, D.R. Tallant, J.A. Voigt, *Appl. Phys. Lett.* **68**, 403 (1996).
9. T. Ohtake, K. Ohkawa, N. Sonoyama, T. Sakata, *J. Alloy. Compd.* **421**, 163 (2006).
10. S.Z. Karazhanov, P. Ravindran, H. Fjellvag, B.G. Svensson, *J. Appl. Phys.* **106**, 123701 (2009).
11. A.L. Stepanov, I.B. Khaibullin, *Rev. Adv. Mater. Sci.* **9**, 109 (2005).
12. Y.Y. Shen, X. Li, Z. Wang, L.L. Zhang, D.C. Zhang, M.K. Li, B. Yuan, Z.D. Li, C.L. Liu, *J. Cryst. Growth* **311**, 4605 (2009).